

Crystallization of chiral compounds

4.* Simple physical model for reconstruction of post-eutectic DSC traces for melting of binary enantiomeric mixtures

D. V. Zakharychev and A. A. Bredikhin*

*A. E. Arbuzov Institute of Organic and Physical Institute, Russian Academy of Sciences,
Kazan Scientific Center of the Russian Academy of Sciences,
8 ul. Akad. Arbuzova, 420088 Kazan, Russian Federation.
Fax: +7 (843) 273 2253. E-mail: dzakhar@iopc.knc.ru*

A theoretical model reproducing qualitative and quantitative characteristics of DSC traces for melting of eutectic enantiomeric mixtures was proposed. The method for reconstruction of an idealized trace from a fragment of the real experimental melting curve was developed. When studying a sample of intermediate enantiomeric composition, the reconstruction of the trace makes it possible to avoid ambiguity in determination of the liquidus temperature, determine the melting temperature for an enantiopure compound, and estimate the composition of the sample.

Key words: differential scanning calorimetry, phase diagram of melting, enantiomers, enantiomeric composition, mephensin.

Phase diagrams form a theoretical basis for many chemical technological processes. Knowledge of peculiarities of phase diagrams of melting and/or dissolution of chiral compounds allows a correct choice of strategy to be chosen for the separation of optical racemates and optimization of purification of the non-racemic product.^{2–4}

Direct experimental information for construction of the phase diagram can be provided by differential scanning calorimetry (DSC). A standard procedure comprises recording of DSC traces for a set of samples of different composition and determination from these traces of the onset and end of melting (solidus and liquidus points, respectively) followed by putting the points in the composition–temperature plot. As applied to mixtures of enantiomers, this general procedure has several specific features. On the one hand, in the liquid phase these systems are close, as a rule, to ideal, which makes it possible to use efficiently the Schröder and Prigogine–Defay equation for their description and thus decrease substantially the amount of experimental material necessary for construction of the phase diagram. On the other hand, for investigation of the type of crystallization of a system under boundary conditions, the construction of phase diagrams requires exact temperature characteristics, whereas the real shape of the DSC trace impedes the precision determination of the liquidus temperature for samples of intermediate composition.

Depending on the specifics of studies, different approaches to processing of DSC traces are used. The physically substantiated linear front model presented, *e.g.*, in Ref. 5, is usually used for melting peaks of a pure individual substance. In this case, the interception point of the tangent to the linear front of the curve with the base line is considered to be the liquidus temperature (coinciding with the solidus temperature for the pure compound that undergoes no phase transitions except for melting). Already for binary systems no single interpretation of the DSC line shape is available. Attempts to develop a general theory of peak shape for thermally initiated events (see, *e.g.*, Ref. 6) have a character of purely mathematical constructions, and their results are virtually inapplicable for analysis of real experimental curves. Another approach is focused on allowance for specific constructional features of a calorimeter and accurate measurement of its time constant accentuated on the correction of instrumental errors caused by sluggishness of the instrument, *etc.*^{7–10} As a rule, DSC traces of pure samples containing the second component as an insignificant admixture can satisfactorily be described by this method. Probably, this approach is efficient and useful for analysis of traces characterizing many events close in the temperature scale, for instance, fast high-temperature phase transitions in the solid phase and non-isothermal kinetics. In some cases, the mathematical model obtained in the framework of this approach for the same instrument is virtually inappropriate for another instrument even close in structure. In the framework of the third approach, the experimental

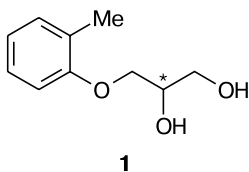
* For Part 3, see Ref. 1.

curve is interpreted as the superposition of curves of several thermally initiated events. In this case, the task is reduced to the decomposition (deconvolution) of a complicated curve to simple (most frequently, using the Gaussian functions) and to obtaining integral characteristics (for example, enthalpy) of individual processes.^{11,12} These procedures are restrictedly applied and inefficient for precision determination of characteristic temperatures of the process.

We know the only work in which the DSC curve shape itself (more exactly, the shape of its ascending part near the completion of melting) was used as an experimental characteristic that provides a possibility to determine purity of the sample under study.¹³ Based on the theoretical equation derived in this work for the shape of the DSC trace of melting of a binary mixture in the concentration region where the properties of the liquid phase are similar to those of an ideal solution, the authors¹³ obtained the so-called "purity function." This function allows the melting run in the region of process completion to be presented as sections of horizontal lines, whose position relative to the ordinate determines the composition of the system. However, processing of the real DSC traces showed that the plots of the "purity function" are nonlinear to a considerable extent. For their linearization, empirical fitting parameters were introduced into the equation which, in combination with the cumbersome character of the expression proposed for the "purity function" itself, decreases substantially appeal of this approach.

In the present work, we attempted to construct a simple model with clear physical meaning reproducing the general features of experimental DSC traces for samples, whose composition lies between the eutectic and pure component. We used the data on melting of 3-(2-methylphenoxy)propane-1,2-diol (**1**) as an experimental material for verification of the theoretical concepts. Compound **1** is a known drug named mephesisin.

We have earlier shown¹⁴ that this chiral compound crystallizes as a conglomerate, *i.e.*, enantiomeric components of the binary mixture are completely mixed in the liquid phase and completely unmixed in the solid phase. The entropy of mixing of the mephesisin enantiomers in the liquid phase determined by us (ΔS_l^m) is $5.24 \text{ J mol}^{-1} \text{ K}^{-1}$ and close to the theoretical value $R \ln 2 = 5.75 \text{ J mol}^{-1} \text{ K}^{-1}$, which implies the absence of enantioselective solvation in the liquid phase. All these data make it possible to consider a mixture of enantiomers of compound **1** as a good approximation to an ideal eutectic binary system. Finally, for conglomerates of chiral compounds the eutectic has the 1 : 1 composition, which allows one to use traces of any nonracemic ("optically active") samples as standard.



Experimental

The syntheses of samples *rac*-**1** (m.p. 69–70 °C (CCl₄)), (*R*)-**1** (m.p. 91–92 °C (CCl₄), $[\alpha]_D^{20} +19.3$ (*c* 1.15, hexane–PrⁱOH (4 : 1))) and (*S*)-**1** (m.p. 91–92 °C (CCl₄), $[\alpha]_D^{20} -19.5$ (*c* 1, hexane–PrⁱOH (4 : 1))) were described in our article.¹⁴ Samples of intermediate composition were prepared by mixing in ethanol of weighed amounts of racemic and scalemic diols **1**; after the solvent was removed and the crystalline precipitate was dried *in vacuo*, the enantiomeric composition (optical purity) of a portion of the sample was determined by polarimetry. Optical rotation was measured on a Perkin–Elmer 341 polarimeter.

Melting curves of samples (~2 mg) were recorded on a Setaram DSC111 modified calorimeter with a heating rate of 1 °C min^{-1} . Peculiarities of apparatus and details of thermographic experiment have been described previously.¹ The enthalpy and melting point of enantiopure compound (*S*)-**1** were $31\,406 \text{ J mol}^{-1}$ and 91.3 °C , respectively.

Results and Discussion

The real DSC traces of melting for chiral samples **1** with different enantiomeric compositions are shown in Fig. 1.

The common characteristic of all curves in the post-eutectic region is the presence of a long descending region at the end of melting after the maximum, because of which the characteristic temperature of this process, *i.e.*, liquidus temperature, cannot unambiguously be determined. It was implicitly supposed¹³ that the curve is diffused due to nonuniformity of the temperature field in the calorimetric cell. Such a nonuniformity should not depend substantially on the sample composition; however, the data in Fig. 1 show that the character of the descent depends strongly on the composition of the system. We

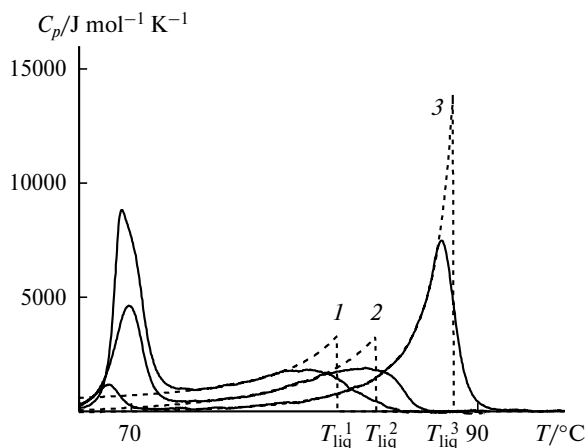


Fig. 1. Experimental (solid lines) DSC traces of melting of samples **1** with different contents of the major enantiomer $x = 0.74$ (**1**), 0.80 (**2**), and 0.94 mole fractions (**3**) and reconstructed (dashed lines) by Eqs (7) and (9) idealized traces for the same samples. For clarifications, see text.

assumed that the diffusion of the curve in the region of process completion is mainly caused by fluctuations of the sample composition over volume due to its discrete character (final size of particles composing the sample). Fluctuations of the composition of sample fragments consisting of discrete particles can be described by the Poisson distribution. However, for many fragments, the number of discrete particles in each of the fragments being rather high in turn, the discrete Poisson distribution can conveniently be approximated by the continuous Gaussian distribution with the parameters $\mu = \bar{x}$, $\sigma = \sqrt{1-\bar{x}}$, where v is the empirical coefficient that characterizes heterogeneity of the mixture under study, and \bar{x} is the averaged composition of the sample expressed in mole fractions. Let us take into account only the composition values \bar{x} for which the fragments of the distribution curves, which are beyond the trace branch considered, can be neglected. Then the thermal effect of sample melting can be determined, as a whole, as the integral value of thermal effects of melting of a set of elementary volumes with the corresponding composition:

$$C_p(T) = \int_{s(T)}^1 f(T, x) \frac{1}{\sqrt{2\pi(1-\bar{x})}} \exp\left[-\frac{(x-\bar{x})^2}{v^2(1-\bar{x})}\right] dx, \quad (1)$$

where $C_p(T)$ is the effective heat capacity of the process at the temperature T ; $s(T)$ is the lower boundary of the composition of elementary volumes yet containing the solid phase at the temperature T ; $f(T, x)$ is the specific heat capacity of melting of the elementary volume; x is the composition of the elementary volume.

Let us consider the AB binary mixture, whose components form no solid solution but form an ideal solution in the liquid state (mixture of stereoisomers forming a racemic conglomerate is, as a rule, a good approximation to similar systems). Let us accept for certainty that the x value in the binary phase diagram of melting changes along the abscissa from 0 to 1. Let a sample of the mixture is taken in an amount of n moles and has the x composition, i.e., the number of components A and B in the whole sample is $n^A = nx$ and $n^B = n(1-x)$, respectively. If the liquidus line for the considered branch of the phase diagram is described by the $x_{\text{liq}}(T)$ function, then according to the lever rule,¹⁵ we can write the equation

$$(n - n_{\text{liq}})/n_{\text{liq}} = (x - x_{\text{liq}})/(1 - x),$$

from which it follows that

$$n_{\text{liq}}(T) = n(1-x)/[1-x_{\text{liq}}(T)]. \quad (2)$$

After differentiating Eq. (2) with respect to temperature, multiplying by the specific melting enthalpy ΔH_A^f of component A, and dividing into the number of

moles n , we have the effective specific heat capacity of the process

$$C_p(T, x) = \frac{\Delta H_A^f (1-x)}{[1-x_{\text{liq}}(T)]^2} \frac{dx_{\text{liq}}(T)}{dT}. \quad (3)$$

In the post-eutectic region, the liquidus curve of the phase diagram for the ideal binary mixture in the elementary volume of the sample under the assumption of infinitely rapidly occurring mass and heat transfer processes is described by the Schröder equation

$$x_{\text{liq}}(T) = \exp\left[\frac{-\Delta H_A^f (T_A^f - T)}{RT_A^f T}\right], \quad (4)$$

where T_A^f is the melting point of the pure component remaining in excess after eutectic melting. After insertion of formula (4) into expression (3), we use the latter as $f(T, x)$ for Eq. (1) and obtain for the specific heat capacity of transformation of the macroscopic AB sample into the liquid phase the resulting formula (Eq. (5)).

$$C_p(T) = \frac{(\Delta H_A^f)^2}{RT^2} \frac{\exp\left[-\Delta H_A^f (T_A^f - T)/(RT_A^f T)\right]}{\left\{\exp\left[-\Delta H_A^f (T_A^f - T)/(RT_A^f T)\right] - 1\right\}^2} \cdot \int_{\exp\left[-\Delta H_A^f (T_A^f - T)/(RT_A^f T)\right]}^1 \frac{1-x}{\sqrt{2\pi(1-\bar{x})}} \exp\left[-\frac{(x-\bar{x})^2}{v^2(1-\bar{x})}\right] dx. \quad (5)$$

The lower integration boundary will be found by the Schröder equation using the concept that to the moment of achieving the T temperature all elementary units with the temperature of the melting end below T have completely transformed into the liquid phase and make no contribution to the effective heat capacity of melting.

The curves (solid lines) calculated by Eq. (5) for samples of different composition of a hypothetical system with the enthalpy and melting point of the pure substance 30 kJ mol⁻¹ and 91 °C, respectively, under the assumption that $v = 0.05$ are shown in Fig. 2.

It is seen that the curve shape is qualitatively consistent with the experimentally observed shape (cf., for example, Fig. 1). The diffusion of the back front increases with an increase in the admixture fraction.

If ignoring heterogeneity of the sample, i.e., assuming that $\sigma = \sqrt{1-\bar{x}} = 0$, the Gaussian of the normal distribution is degenerate to the Dirac delta function. As a result of integration of the latter, the Φ function (Heaviside switching function) appears in the expression and Eq. (5) takes the form of Eq. (6).

$$C_p(T) = (x-1) \frac{(\Delta H_A^f)^2}{RT^2} \frac{\exp\left[-\Delta H_A^f (T_A^f - T)/(RT_A^f T)\right]}{\left\{\exp\left[-\Delta H_A^f (T_A^f - T)/(RT_A^f T)\right] - 1\right\}^2} \cdot \Phi\left(\frac{-\Delta H_A^f T_A^f}{-\Delta H_A^f + \ln(x) RT_A^f} - T\right). \quad (6)$$

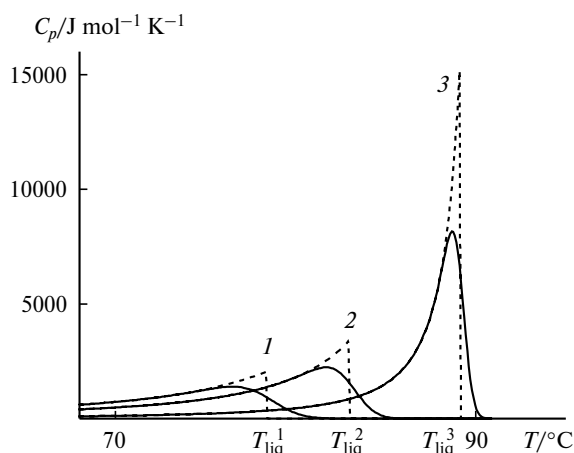


Fig. 2. Theoretical melting curves for the hypothetical systems of different composition ($x = 0.7$ (1), 0.8 (2), and 0.95 (3)) with allowance for (solid lines) and ignoring (dashed lines) heterogeneity of the sample composition. For clarifications, see text.

Dashed lines in Figs 2 were obtained by the calculation assuming no heterogeneities in the sample composition. According to Eq. (6), termination of the curves (achievement of the base line) occurs after the solid phase fraction has completely disappeared in the system, *i.e.*, after achieving the liquidus temperature T_{liq} for a sample of certain composition. Note that no visually distinguished point corresponds to this temperature in the solid curves that simulate the real experiment and were plotted with allowance for heterogeneity of the sample composition. Expression (6) is similar to the equation for the heat flow proposed earlier.¹³

When comparing the solid and dashed lines in Fig. 2, it becomes evident that heterogeneity of the sample affects substantially only the stage of melting completion and exerts virtually no effect on the shape of the ascending branch of the experimental curve in the region rather remote from eutectic melting. Therefore, the monotonic ascending region in the experimental DSC trace can be used for reconstruction of the entire contour of curves of type (6) by fitting of the region of the theoretical curve to the corresponding fragment of the experimental curve using nonlinear regression methods. Expression (6) is cumbersome and not very convenient for practical use but the term

$$\frac{\exp\left[-H_A^f(T_A^f - T)/(RT_A^f T)\right]}{\left\{\exp\left[-H_A^f(T_A^f - T)/(RT_A^f T)\right] - 1\right\}^2}$$

is efficiently interpolated by the fractional rational function for the Loran series expansion

$$\frac{e^{-z}}{(1 - e^{-z})^2} \approx \frac{1}{z^2} + \dots$$

in the vicinity of $z = 0$, *i.e.*, at $T_A^f \approx T$. In this case, the series of expansion terms is mutually annihilated: for

the series contracted to the first four elements we obtain the single nonzero coefficient at z^{-2} . The relative error of this interpolation for the calculation of heat flows by the simplified formula in the already studied hypothetical system (see Fig. 2, dashed curves) in the temperature interval $T_A^f - T \leq 20$ is at most $5 \cdot 10^{-3}$. The expression (ignoring the term corresponding to the Heaviside function) takes the form convenient for practical calculations

$$C_p(T) = (1 - x)R(T_A^f)^2/(T_A^f - T)^2. \quad (7)$$

This result seems paradoxical, because Eq. (7) describing the peak shape of sample melting contains no enthalpy of the process. Moreover, when normalizing the temperature scale to the melting point of the predominant component and the ordinate to the content of a minor component $(1 - x)$ in the system, Eq. (7) can be written in the form demonstrating that the melting trajectories of ideal binary systems are unified in the post-eutectic region:

$$C_p(T)/(1 - x) = R(1 - T/T_A^f)^{-2}. \quad (8)$$

To verify this conclusion, we calculated using the complete equation (5) the fragments of melting trajectories of hypothetical binary systems with coinciding composition and melting point of the predominant component but with substantially different melting enthalpies. As can be seen from the data in Fig. 3, the ascending branches of the calculated traces coincide in fact and, hence, the simplified expression (7) containing no enthalpy terms can be used for approximation of the idealized DSC trace by the shape of the ascending fragment of the experimental curve.

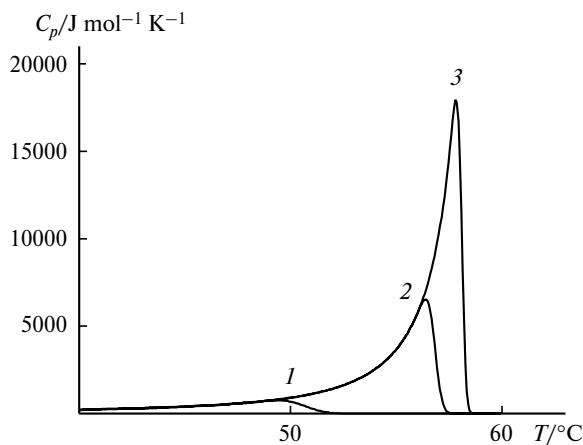


Fig. 3. Melting curves of the hypothetical crystalline samples with $T_A^f = 60$ °C containing the major component $x = 0.9$ and melting enthalpies 10 (1), 30 (2) and 50 kJ mol⁻¹ (3).

Table 1. Parameters of the reconstructed melting curves and related characteristics of mephnesin samples **1**

Curve	T_{liq} /°C	Parameters of reconstructed curve		x^*		
				I	II	III
		a	b ($b - 273.2$)			
1	81.9	0.40	365.8 (92.6)	0.74	0.60	0.73
2	84.5	0.24	365.7 (92.5)	0.80	0.76	0.78
3	88.6	0.06	364.0 (90.8)	0.94	0.94	0.94

* Mole fraction of the predominant enantiomer according to the polarimetry data (I), determined from the expression $1 - a$ (II), and calculated using the Schröder equation (III).

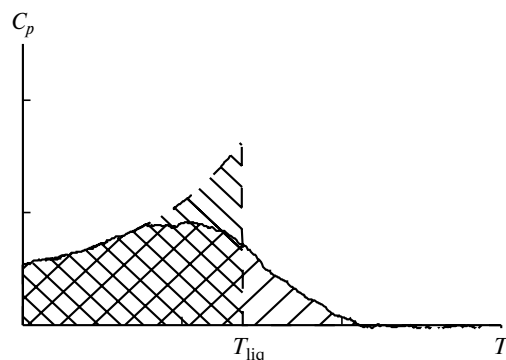
The following expression is used in practice to reconstruct theoretical curves from fragments of experimental traces:

$$C_p(T) = Ra/(1 - T/b)^2 - c, \quad (9)$$

where $a = 1 - x$, $b = T_A^f$; the additional parameter c makes it possible to compensate inaccuracies in determination of the base line. In the present work, the coefficients were determined by the nonlinear regression method, and only the monotonically increasing fragments of the experimental traces were used in the procedure. Thus reconstructed idealized melting curves for the nonracemic samples of diol **1** are presented in Fig. 1 (dashed lines). The a and b parameters for each curve are given in Table 1.

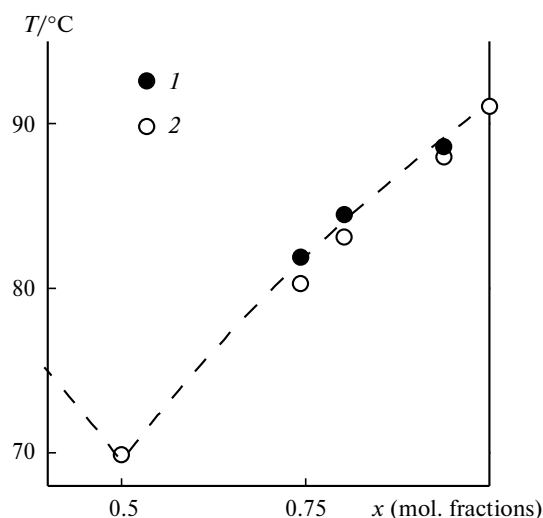
First, a comparison of the reconstructed and experimental DSC traces makes it possible to determine the characteristic point of melting end T_{liq} with a minimum arbitrariness. The reconstructed curve (9) reproduces the idealized trace (6) (see Fig. 2), and the surface area under the curve equals the melting enthalpy of the sample. Then it seems natural to accept as T_{liq} the point at which the surface area under the reconstructed curve becomes equal to that under the experimental melting curve corresponding to the observed melting enthalpy of the sample (Fig. 4).

The dashed curves in Fig. 1 terminate in points determined according to the described procedure; thus determined T_{liq} are given in Table 1. The fragment of the phase diagram for melting of diol **1** is shown in Fig. 5. The dashed line corresponds to the liquidus line calculated by the Schröder equation (4) based on the data for the pure enantiomer, 1 are temperatures of melting end experimentally determined by the method of reconstructed curve termination (see Table 1), and 2 are the maxima of the experimental melting curves (80.3, 83.1, and 88.0 °C, respectively). It is seen that the first set is better consistent with the theory. Note that the proposed procedure is objective, whereas the determination of the maximum in flat curves (and other empirical procedures described in literature) assumes voluntary or involuntary arbitrariness in

**Fig. 4.** Experimental (solid line) and reconstructed by formula (9) (dashed line) DSC traces. The point in which the surface area under the calculated curve becomes equal to the surface area under the experimental curve corresponds to the temperature of melting end (termination of the reconstructed curve).

finding experimental parameters. It seems that the procedure of reconstructed curve termination is also efficient for systems far from ideality. In this case, the approximating curve can be considered as an empirical function that aligns diffusion of the back front of the melting peak; an increase in the steepness of the theoretical curve with approaching to the cut-off point decreases the sensitivity of the determined liquidus temperature to deviations from ideality. Naturally, the physical meaning of the a and b coefficients can be lost.

For the systems close to ideality, the a parameter, which is determined from the nonlinear regression and characterizes the content of the minor component, is very sensitive to the accuracy of determination of the base line

**Fig. 5.** Calculated liquidus line for mephnesin **1** and points of melting end for the samples of different composition determined experimentally: 1, by the method of reconstructed curve termination (see Table 1) and 2, by the maxima of the experimental melting curves.

and distortions of the curve shape due to both instrumental errors and trace amounts of admixtures of the third components in the sample. However, the reconstruction of an ideal contour provides other possibilities. First, the accurate determination of the melting end temperature of the sample T_{liq} allows one to calculate the composition directly from the Schröder equation (4). The ΔH_A^f value necessary for this purpose should be estimated from the total integral surface area of the melting trace of the most pure sample in the series under study. The melting temperature of the pure sample T_A^f can be determined directly from experiment or estimated using the calculated parameter $b = T_A^f$. It is clear that the use of the experimental trace for the most pure sample is preferential in this case. The estimates of the enantiomeric purity of samples **1** obtained using the both approaches are given in Table 1. Evidently, the accuracy of determination of the enantiomeric composition directly from the regression parameter increases with an increase in the enantiomeric purity and can be considered for a sample with moderate enantiomeric excess only as an approximate estimate. At the same time, the use of the Schröder equation allows one to monitor the composition with a sufficient accuracy in the whole interval under study.

As a whole, the procedure proposed for reconstruction of the ideal melting curve by the fragment of the contour of the experimental DSC trace can be a convenient alternative to the earlier proposed method.¹³ For binary mixtures of enantiomers, the proposed approach makes it possible to restrict arbitrariness in determination of the temperature of melting end of the sample, estimate the enantiomeric purity and melting point of the pure substance from the single experimental trace of a sample with the unknown beforehand composition, and analyze with sufficient accuracy the enantiomeric purity of the sample virtually in the whole interval of compositions.

This work was financially supported by the Russian Foundation for Basic Research (Project No. 06-03-32508)

and the Division of Chemistry and Materials Science of the Russian Academy of Sciences (Program for Fundamental Research No. 4.2).

References

1. D. V. Zakharychev, S. N. Lazarev, Z. A. Bredikhina, and A. A. Bredikhin, *Izv. Akad. Nauk, Ser. Khim.*, 2006, 225 [*Russ. Chem. Bull., Int. Ed.*, 2006, **55**, 230].
2. J. Jacques, A. Collet, and S. H. Wilen, *Enantiomers, Racemates, and Resolutions*, Krieger Publishing Co, Malabar, FL, 1994, 447 pp.
3. E. L. Eliel, S. H. Wilen, and L. N. Mander, *Stereochemistry of Organic Compounds*, John Wiley and Sons, New York, 1994, 1267 pp.
4. Y. Wang, R. LoBrutto, R. W. Wenslow, and I. Santos, *Org. Proc. Res. Dev.*, 2005, **9**, 670.
5. G. W. H. Höhne, H. K. Cammenga, W. Eysel, E. Gmelin, and W. Hemminger, *Thermochim. Acta*, 1990, **160**, 1.
6. U. B. Cepidor, E. Brizzi, R. Bucci, and A. D. Magri, *Thermochim. Acta*, 1994, **247**, 347.
7. S. Sarge, S. Bauerecker, and H. K. Cammenga, *Thermochim. Acta*, 1988, **129**, 309.
8. J. E. K. Schawe, *Thermochim. Acta*, 1993, **229**, 69.
9. S. W. Chen, Ch. Ch. Huang, and J. Ch. Lin, *Chem. Eng. Sci.*, 1995, **50**, 417.
10. R. L. Danley, *Thermochim. Acta*, 2004, **409**, 111.
11. M. Elsabee and R. J. Prankerd, *Int. J. Pharmaceutics*, 1992, **86**, 211.
12. R. F. Speyer, *J. Mater. Res.*, 1993, **8**, 675.
13. R. J. Bader, J. E. K. Schawe, and G. W. H. Höhne, *Thermochim. Acta*, 1993, **229**, 85.
14. A. A. Bredikhin, Z. A. Bredikhina, S. N. Lazarev, and D. V. Savel'ev, *Mendeleev Commun.*, 2003, 104.
15. A. G. Stromberg and D. P. Semchenko, *Fizicheskaya khimiya [Physical Chemistry]*, Vysshaya Shkola, Moscow, 2001, p. 168 (in Russian).

Received May 22, 2006;
in revised form December 15, 2006